Prognostic Significance and Functional Role of CEP57 in Prostate Cancer[1]

Josef Mang*, Nina Korzeniewski*, Dimo Dietrich[†], Verena Sailer[†], Yanis Tolstov*, Sam Searcy*, Jost von Hardenberg[‡], Sven Perner[§], Glen Kristiansen[†], Alexander Marx[¶], Wilfried Roth[#], Esther Herpel[#,**], Carsten Grüllich[††], Valentin Popeneciu[‡‡], Sascha Pahernik[‡‡], Boris Hadaschik[‡‡], Markus Hohenfellner[‡‡] and Stefan Duensing*,[‡‡]

*Molecular Urooncology, Department of Urology, Medical Faculty Heidelberg, University of Heidelberg, Im Neuenheimer Feld 517, D-69120 Heidelberg, Germany; [†]Institute of Pathology, University of Bonn School of Medicine, Sigmund-Freud-Strasse 25, D-53127 Bonn, Germany; [‡]Department of Urology, Medical Faculty Mannheim, University of Heidelberg, Theodor-Kutzer-Ufer 1-3, D-68167 Mannheim, Germany; [§]Pathology Network of the University Hospital of Lübeck and Leibniz Research Center Borstel, Ratzeburger Allee 160, D-23538 Lübeck, Germany; [¶]Institute of Pathology, Medical Faculty Mannheim, University of Heidelberg, Theodor-Kutzer-Ufer 1-3, D-68167 Mannheim, Germany; [#]Institute of Pathology, University of Heidelberg School of Medicine, Im Neuenheimer Feld 224, D-69120 Heidelberg, Germany; [**]Tissue Bank of the National Center for Tumor Diseases (NCT), Im Neuenheimer Feld 220/221, D-69120 Heidelberg, Germany; [††]National Center for Tumor Diseases (NCT), Department of Medical Oncology, Im Neuenheimer Feld 460, D-69120 Heidelberg, Germany; [‡‡]Department of Urology, University of Heidelberg School of Medicine, Im Neuenheimer Feld 110, D-69120 Heidelberg, Germany

Abstract

We have recently shown that centrosomal protein 57 (CEP57) is overexpressed in a subset of human prostate cancers. CEP57 is involved in intracellular transport processes, and its overexpression causes mitotic defects as well as abnormal microtubule nucleation and bundling. In the present study, we further characterized the prognostic and functional role of CEP57 in prostate cancer. Unexpectedly, we found that high CEP57 expression is an independent prognostic factor for a more favorable biochemical recurrence-free survival in two large patient cohorts. To reconcile this finding with the ability of CEP57 to cause cell division errors and thus potentially promote malignant progression, we hypothesized that alterations of microtubule-associated transport processes, in particular nuclear translocation of the androgen receptor (AR), may play a role in our finding. However, CEP57 overexpression and microtubule bundling had, surprisingly, no effect on the nuclear translocation of the AR. Instead, we found a significant increase of cells with disarranged microtubules and a cellular morphology

suggestive of a cytokinesis defect. Because mitotic dysfunction leads to a reduced daughter cell formation, it can explain the survival benefit of patients with increased CEP57 expression. In contrast, we show that a reduced expression of CEP57 is associated with malignant growth and metastasis. Taken together, our findings underscore that high CEP57 expression is associated with mitotic impairment and less aggressive tumor behavior. Because the CEP57-induced microtubule stabilization had no detectable effect on AR nuclear translocation, our results furthermore suggest that microtubule-targeting therapeutics used in advanced prostate cancer such as docetaxel may have modes of action that are at least in part independent of AR transport inhibition.

Translational Oncology (2015) 8, 487–496

Introduction

Prostate cancer is the most commonly diagnosed noncutaneous malignancy in men in developed countries. Prostate cancer is the second leading cause of male cancer-related death in the United States and the third leading cause in Europe [1].

Although prostate-specific antigen (PSA) screening has resulted in a decrease of prostate cancer–related mortality [2], this major achievement comes at the cost of overtreatment of indolent tumors. It is hence of paramount importance to identify markers that can help to further define subgroups of patients for a risk-adapted, individualized treatment.

Prostate cancer is characterized by chromosomal instability including aneuploidy [3]. Aneuploidy is frequently caused by cell division errors [4] due to centrosome amplification, and such aberrations are likewise frequently detected in prostate cancer [5].

We have recently shown that the centrosomal protein 57 kDa (CEP57) is overexpressed in a subset of prostate cancers [6]. CEP57 has an N-terminal centrosome localization and multimerization domain and a C-terminal microtubule-binding and stabilization domain [7]. CEP57 was first described as a mediator of microtubule-dependent internalization and nuclear trafficking of the 18-kDa isoform of fibroblast growth factor type 2 (FGF-2, basic FGF) [8]. CEP57 has been shown to be critically involved in FGF-2-induced centrosome overduplication, and ectopic expression of CEP57 alone has been demonstrated to induce centriole overduplication and mitotic instability [6]. CEP57 overexpression also leads to a stabilization of microtubules and a striking formation of microtubule bundles that have been referred to as "basket" structures [7].

Growth and differentiation of the prostate gland during development are dependent on androgens, and prostate cancers are also initially androgen dependent [9]. Androgen signaling is mediated through the androgen receptor (AR), a ligand-activated transcription factor. Targeting the androgen-AR axis by androgen deprivation therapy (ADT) therefore represents the first-line therapy for advanced prostate cancer [10]. Although most patients with advanced prostate cancer initially respond to ADT, they ultimately develop resistance leading to a metastatic castration-resistant stage (mCRPC) [11]. Despite circulating androgens at castrate level, castration-resistant prostate cancer cells still critically depend on androgen signaling, and a number of mechanisms have been identified that maintain these signaling cues [12–14]. Patients with mCRPC are frequently treated with docetaxel, a microtubule-stabilizing drug that is believed to function through its antimitotic

effects and, in a typically slowly growing tumor such as prostate cancer, other mechanisms such as inhibition of the microtubule-dependent nuclear translocation of the AR [15].

In the present study, we show that high CEP57 expression characterizes a subset of prostate cancer patients with a more favorable prognosis. We attribute this finding to a growth-suppressive effect of CEP57 overexpression that involves a failure to produce daughter cells due to impaired cell division. In contrast to our initial hypothesis, a blockade of the nuclear translocation of the AR caused by microtubule bundling appears not to play a role in the more favorable prognosis of patients with CEP57 overexpression. These findings have a number of translational implications for the prognosis and treatment of prostate cancer.

Material and Methods

Cell Culture, Transfections, and Drug Treatment

Human prostate cancer cell lines LNCaP and PC-3 and mouse NIH3T3 cells were obtained from CLS Cell Line Service (Eppelheim, Germany) and maintained according to the distributor's recommendations. For transient DNA transfection, the following plasmids were used: murine (m)CEP57-myc-flag (kindly provided by Ko Momotani University of Virginia, Charlottesville, VA) [7], pCMV6-myc-flag empty vector (Origene, Rockville, MD), centrin-GFP (kindly provided by Michel Bornens, Institut Curie, Paris, France) [16], mitochondrial DsRed (Clontech, Mountain View, CA), and AR-C1-pEGFP and C1-pEGFP empty vector (Addgene, Cambridge, MA). LNCaP and PC-3 cells were transfected using the Neon Transfection System (Life Technologies, Carlsbad, CA) according to instructions provided by the manufacturer. Briefly, 70% to 90% confluent cells were harvested and then washed twice with PBS. LNCaP cells, mixed with plasmid DNA, in a 100-µl Neon tip were electroporated at 1250 V, 2 × 20–millisecond pulse length. PC-3 cells, mixed with plasmid DNA, in a 100-µl Neon tip were electroporated at 1250 V, 30-millisecond pulse length. NIH3T3 cells were transfected using lipofection (Fugene; Promega, Madison, WI). To induce AR nuclear translocation, cells were treated with 5 nM R1881 or DMSO as control for 2 hours and analyzed thereafter by fluorescence microscopy.

Antibodies

The following antibodies were used: mouse anti-CEP57 (Abcam, Cambridge, UK), rabbit anti-AR, rabbit anti-FGF2, mouse anti-α-tubulin (all from Santa Cruz, Santa Cruz, CA), rabbit anti-myc-tag (Cell

Signaling, Danvers, MA), mouse anti-p63 (GeneTex, Irvine, CA), mouse anti-Ki67 (Dako, Glostrup, Denmark), and rabbit anti–fibroblast growth factor receptor 1 (FGFR1) (Sigma-Aldrich, St. Louis, MO).

Immunofluorescence Microscopy

Cells were grown on coverslips, fixed in 4% paraformaldehyde/PBS for 10 minutes at room temperature, washed with PBS, permeabilized with 1% Triton-X100/PBS for 10 minutes at room temperature, and washed in PBS. Fixed cells were then incubated with primary antibody diluted in PBS at 4°C overnight. Dilutions for primary antibodies were as follows: anti-myc-tag (1:200) and anti-α-tubulin (1:200). The following day, cells were incubated for 2 hours at room temperature with secondary antibody Alexa Fluor 488 or Alexa Fluor 555 (Life Technologies) diluted 1:1000 in PBS and then again washed with PBS. Finally, cells were mounted with DAPI-containing mounting medium (Vectashield; Vector Laboratories, Burlingame, CA). Cells were analyzed using a Leica DM5000B fluorescence/brightfield microscope.

Immunohistochemistry

Patient-derived tumor specimens were collected under approval by the Ethics Committee of the Medical Faculty of the University of Bonn (071/14), the Medical Faculty Heidelberg of the University of Heidelberg (206/2005, 207/205, S-085/2012), and the Medical Faculty Mannheim of the University of Heidelberg (2012-229N-MA). Tissue samples from the tissue bank of the National Center for Tumor Diseases Heidelberg were provided in accordance with the regulations of the tissue bank and the approval of the Ethics Committee of the University of Heidelberg. Two tissue microarrays (TMAs) were used in this study: TMA I was obtained commercially (TriStar Technology Group, Washington, DC), and TMA II was constructed by the Institute of Pathology of the University of Bonn. Age, PSA at diagnosis, and TNM status were comparable between the two TMAs. However, TMA I contained only 1.2% of tumors with a Gleason score >7 in comparison to 21.2% in TMA II. Information about adjuvant treatment was not available for TMA I. A total of 45 of 212 patients of the TMA II cohort received adjuvant radiotherapy. There was no statistical difference between patients with adjuvant radiotherapy and without radiotherapy with respect to CEP57 staining (P = .18; chi-square). Briefly, paraffin-embedded tissue was incubated overnight at 37°C. Next day, the slides were deparaffinized by incubating in xylene for 12 minutes followed by a graded ethanol series (100%, 90%, and 70% for 4 minutes each). Antigen retrieval was performed using a steamer for 30 minutes and target retrieval solution (Dako) diluted 1:10 in dH$_2$O. Primary antibodies were incubated at 4°C overnight diluted in PBS using the following dilutions: anti-CEP57 (1:100), anti-p63 (1:75), anti-AR (1:100), anti-FGF-2 (1:100), anti-FGFR1 (1:100), and anti-Ki-67 (1:100). Immunodetection was performed using the HistostainPlus kit (Life Technologies) according to manufacturer's recommendations.

3-(4,5 Dimethyldiazol-2-yl)-2,5 Diphenyltetrazolium Bromide (MTT) Assay

Cells were grown in 60-mm tissue culture plates, and the Vybrant MTT Cell Proliferation Assay kit (Life Technologies) was used according to manufacturer's instructions. Briefly, 12 mM MTT stock solution was prepared using 1 ml of PBS for each vial of MTT. MTT stock solution then was diluted 1:10 in cell culture media, and cells were incubated for 4 hours at 37°C. After 4 hours, 10 mM HCl containing 0.1 g/ml of SDS was added to the MTT-containing media to a final dilution of 1:1. Cells were then incubated for 18 hours at 37°C before measuring absorbance at 570 nm with the Glomax Multi luminometer (Promega, Madison, WI).

Statistical Methods

Associations between clinicopathological variables and CEP57 protein expression were analyzed using the Kendall τ rank correlation, χ^2 test, or Fisher exact probability test. Student's two-tailed t test for independent samples was performed wherever appropriate. Biochemical recurrence (BCR)-free survival was calculated using the Kaplan-Meier method, and survival time differences were compared using the log-rank test. CEP57 expression was also examined within univariate and multivariate Cox proportional hazards regression models. P values refer to the Wald test. P values <.05 were considered to be statistically significant. All analyses were carried out using the SPSS software package (IBM, Armonk, NY).

Results

CEP57 Overexpression and Biochemical Recurrence-Free Survival of Prostate Cancer Patients

We have previously reported that CEP57 is overexpressed in a subset of prostate cancers, whereas normal tissue consistently shows no or a weak to moderate expression [6]. However, a correlation to patient survival was not possible in our earlier study because of a lack of clinical follow-up information. Here, we addressed this question by first staining a commercially available TMA containing 500 prostate cancer samples with survival data for CEP57 by immunohistochemistry. A total of 341 out of 500 cores were evaluable for scoring of CEP57 expression (J.M. and S.D.). We found that 186 of 341 (55%) samples showed a high CEP57 expression, whereas 155 of 341 (45%) showed a low (negative or weak to moderate) expression of CEP57 (Suppl. Table 1; Figure 1, A and B). Kaplan-Meier analysis revealed a trend toward a more favorable BCR-free survival for patients with high CEP57 expression compared with patients with low CEP57 expression over a 60-month follow-up period (log-rank, P < .05; Figure 1B).

We next sought to confirm our findings using a second, independent TMA constructed at the University of Bonn Medical School (V.S., D.D., G.K.). A total of 212 patient specimens were scored for CEP57 expression after immunohistochemical staining. Absence of CEP57 was detected in 1 of 212 specimens (0.3%), 72 of 212 samples showed a weak CEP57 expression (24%), moderate expression was found in 104 of 212 samples (34.7%), whereas 35 of 212 specimens showed a high CEP57 expression (11.7%; Suppl. Table 2). Kaplan-Meier analysis of this second patient cohort confirmed a significantly better BCR-free survival for patients with tumors showing high CEP57 expressing compared with patients with lower expression (log-rank, P = .006; Figure 1C). We next performed a univariate and multivariate Cox analysis (Table 1). The N stage was not prognostic because of the small number of N1 patients (14/212). Pathological T stage and Gleason score were both significant prognosticators in the univariate analysis, whereas the T stage lost its significance in the multivariate analysis because of its association with the Gleason score. Importantly, however, we found that CEP57 was an independent prognostic factor for BCR-free patient survival (Table 1).

CEP57 Overexpression Impairs Cell Viability In Vitro Independent of AR Nuclear Transport

To determine possible biological mechanisms involved in the more favorable BCR-free patient survival associated with high CEP57 expression, a number of in vitro experiments were performed. We first overexpressed CEP57 in prostate cancer cells and analyzed CEP57 and α-tubulin staining by co-immunofluorescence microscopic analysis to test its functionality. We readily detected "basket" structures [7]
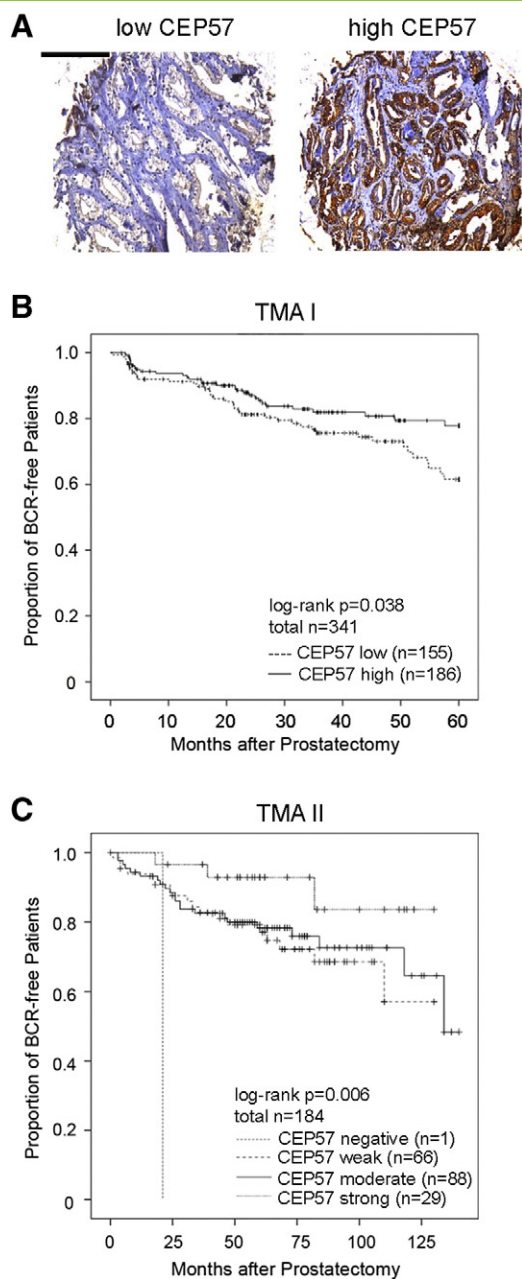
Figure 1. High CEP57 expression is associated with more favorable BCR-free survival in two cohorts of prostate cancer patients. (A) Examples of immunohistochemical staining for CEP57 in two prostate cancer specimens with low or high protein expression, respectively. Scale bar = 250 μm. (B, C) Kaplan-Meier curves of BCR-free survival using two TMAs either obtained commercially (TMA I) or collected at the University of Bonn School of Medicine (TMA II). The log-rank test was used to calculate P values.

Table 1. Univariate and Multivariate Cox Proportional Hazard Model Analyses on BCR-Free Survival for CEP57 Protein Expression, Gleason, pT, Preoperative PSA Level, Surgical Margin, and Nodal Status

	Univariate Cox Analysis		Multivariate Cox Analysis	
	Hazard Ratio [95% CI]	P Value	Hazard Ratio [95% CI]	P Value
Pathological stage (pT$_2$ reference)				
pT$_3$ and pT$_4$	2.15 [1.18-3.92]	.012	1.11 [0.56-2.19]	.76
Gleason sum (7 reference)				
<7	0.33 [0.14-0.81]		0.28 [0.11-0.72]	
>7	3.854 [1.89-7.85]	<.001	3.22 [1.51-6.86]	<.001
Nodal status (N$_0$ reference)				
N$_1$	1.16 [0.45-3.54]	.66	0.50 [0.14-1.77]	.28
Surgical margin (R$_0$ reference)				
R$_1$	1.89 [1.03-3.47]	.039	2.03 [1.03-3.99]	.041
Preoperative PSA	1.01 [0.99-1.02]	.47	1.00 [0.98-1.02]	.96
CEP57	0.63 [0.40-0.99]	.045	0.55 [0.32-0.92]	.022

Gleason score was analyzed as categorized (<7, 7, and >7) variable. Preoperative PSA level was analyzed as continuous variable.

statistically significant reduction of cell viability was found in CEP57-overexpressing cells compared with control-transfected cells (88.8% normalized to controls; P < .001). This decrease of viability was in the range of cells treated with 50 nM docetaxel (76.5%; P < .0001). A combination of CEP57 overexpression and docetaxel treatment led to a further reduction of cell viability (67.8%; P < .0001). These results underscore that high CEP57 expression impairs the viability of prostate cancer cells to a similar extent than docetaxel.

CEP57 has previously been implicated in a number of potentially oncogenic mechanisms related to aberrant microtubule and/or centrosomal functions [6,8,17]. However, because we detected a more favorable effect on patient survival and reduced viability of prostate cancer cells *in vitro* upon overexpression, we hypothesized that other functions of CEP57 may override potentially pro-oncogenic properties. To this end, we postulated that the microtubule-bundling function of CEP57 may interfere with nuclear transport of the AR. This process is essential for prostate cancer cell viability, and interference with AR trafficking has been implicated in the mode of action of anticancer agents used in prostate cancer including taxanes and enzalutamide [18,19].

To examine this notion, we used an AR transport assay on the single-cell level using a plasmid that expresses AR tagged with green fluorescent protein (AR-GFP). We transiently transfected PC-3 cells, which do not express the AR physiologically, with AR-GFP or GFP control plasmid, respectively (Figure 4). We then determined AR nuclear transport following stimulation of cells with the synthetic androgen R1881 or DMSO as control. Treatment with R1881 resulted in a robust nuclear relocalization of AR-GFP, whereas DMSO treatment did not induce nuclear translocation (Figure 4).

To examine AR translocation in the presence or absence of CEP57 overexpression, we transfected PC-3 cells with AR-GFP plus CEP57 or AR-GFP plus empty vector as control, respectively, and stimulated the cells with R1881 or DMSO (Figure 5). Surprisingly, CEP57 overexpression did not block AR-GFP translocation to the nucleus despite a clearly detectable induction of microtubule bundles (Figure 5A). To rule out that this finding was not due to the fact that PC-3 cells lack AR expression, we repeated this experiment in hormone-sensitive LNCaP cells that harbor a mutated AR and observed the same result as in PC-3 cells (Figure 5B). Taken together, these findings suggest that CEP57-induced microtubule bundling does not block microtubule-mediated AR translocation to the nucleus.
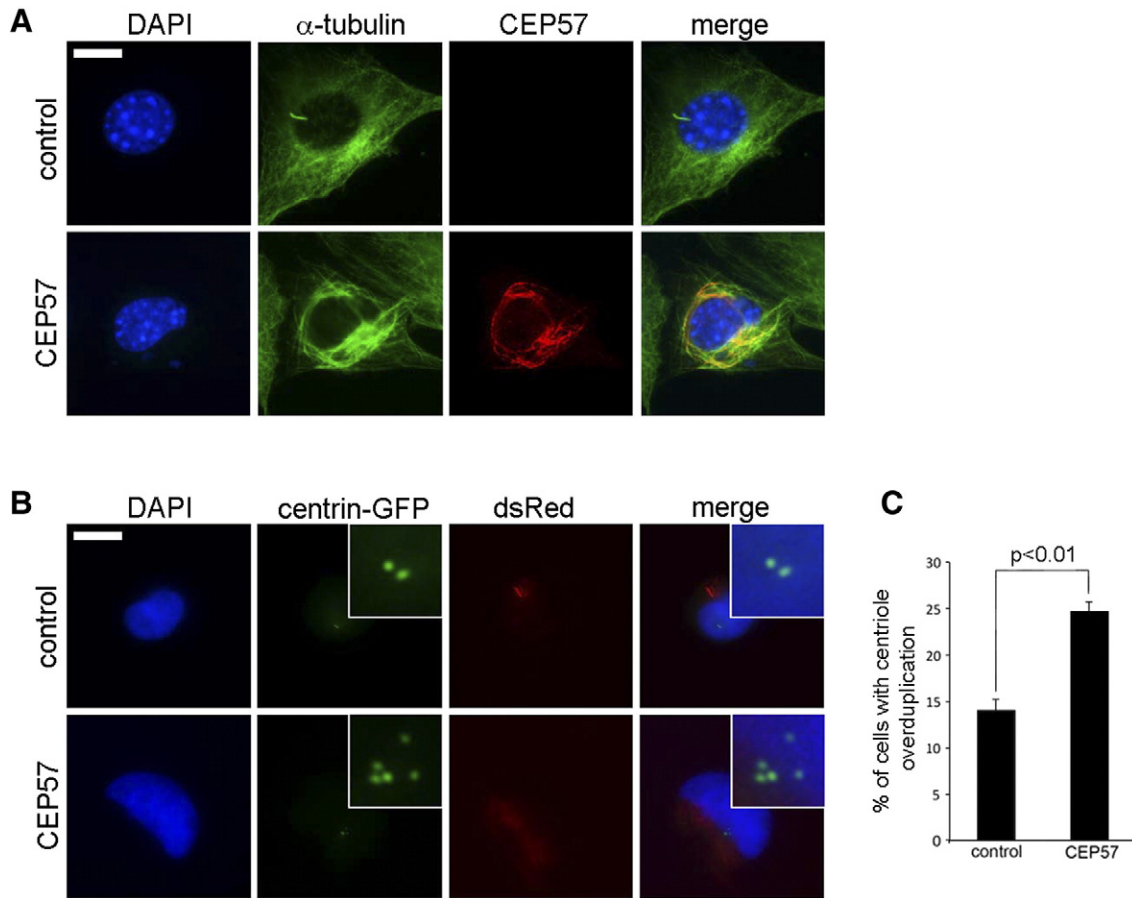
consisting of α-tubulin–positive microtubule bundles colocalizing with CEP57, whereas such structures were absent in control-transfected cells (Figure 2A). To further verify that CEP57 was functional, we also showed that transient overexpression induced centriole overduplication as previously reported (Figure 2, B and C) [6].

We next investigated the effect of CEP57 overexpression on cell viability. LNCaP cells were transiently transfected with either a control plasmid or a CEP57 expression plasmid, and cell viability was measured after 48 hours using the MTT assay (Figure 3). A moderate but

Figure 2. CEP57 overexpression induces microtubule bundling and promotes centriole overduplication. (A) Co-immunofluorescence microscopic analysis of CEP57 and α-tubulin to visualize CEP57-induced microtubule bundles ("basket") in mouse NIH3T3 cells overexpressing either empty vector (control) or murine (mCEP57). Nuclei stained with DAPI. Scale bar = 10 μm. (B) Immunofluorescence microscopic analysis of centrioles in LNCaP cells expressing centrin-GFP as a centriole marker and transfected with either empty vector (control) or mCEP57. A DsRed encoding plasmid was used as transfection control. Nuclei stained with DAPI. Scale bar = 10 μm. (C) Quantification of overduplicated centrioles (>4 centrioles per cell, >1 daughter at a single maternal centriole) in LNCaP cells transfected with centrin-GFP together with an empty vector (control) or mCEP57. Statistical analysis was performed using Student's two-tailed t test for independent samples.
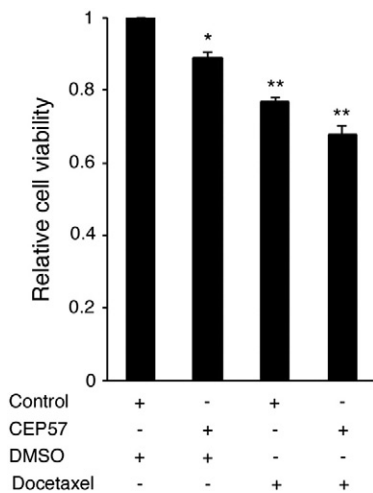

Figure 3. Overexpression of CEP57 is growth suppressive. MTT assay measuring viability of LNCaP cells either 48 hours after transfection with empty vector (control) or mCEP57 alone or with docetaxel at a 50-nM concentration. *P < .001, **P < .0001 (Student's two-tailed t test for independent samples).

CEP57 Overexpression Does Not Block AR Nuclear Localization In Vivo

We next investigated whether high CEP57 expression interferes with AR transport *in vivo* in primary prostate cancer specimens. Directly adjacent tissue sections from 18 prostate cancers were stained for CEP57 or AR by immunohistochemistry (Figure 6A). Of the samples stained, 6 (33.3%) showed a high CEP57 expression, whereas 12 showed a low CEP57 expression (66.7%, Figure 6B). Staining for AR was positive in all tumors, with 14 showing strictly nuclear AR expression (77.8%) and 4 presenting with both nuclear and cytoplasmic AR staining (22.2%; P > .05).

CEP57 Is Frequently Overexpressed in Prostate Basal Cells

While examining CEP57 expression in these samples, we discovered that CEP57 was highly overexpressed in areas of prostate basal cell hyperplasia (Figure 7). To confirm that CEP57-overexpressing cells were indeed basal cells, we co-stained prostate samples with CEP57 and the basal cell marker p63, which is typically not expressed in other prostate cell types including luminal and tumor cells [20]. To further characterize basal cells with CEP57 overexpression, we also stained for FGF-2 and FGFR1 because CEP57 plays an important role in FGF-2 signaling
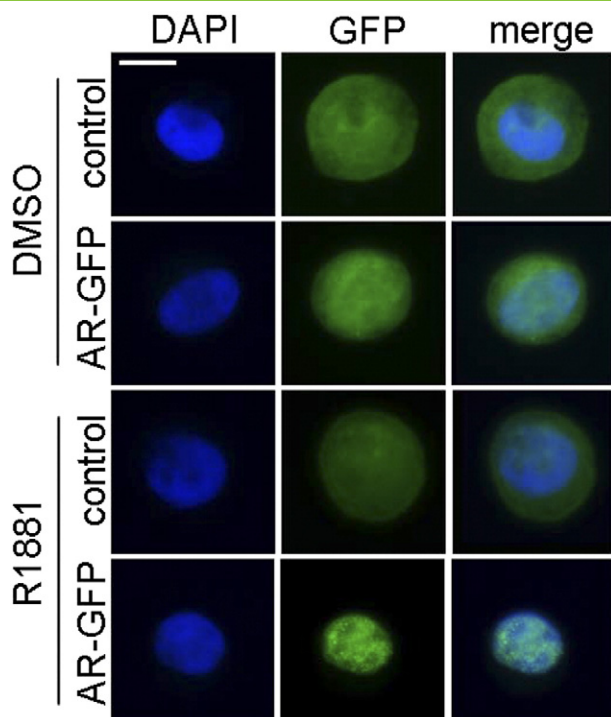
Figure 4. AR transport assay. Fluorescence microscopic analysis of PC-3 cells following transfection with either a GFP-expressing empty vector (control) or AR-GFP. Twenty-four hours after transfection, cells were treated with either 5 nM R1881 or DMSO as a control (2 hours) to induce AR nuclear translocation. Note the virtually complete nuclear translocation of AR-GFP after R1881 stimulation. Nuclei stained with DAPI. Scale bar = 10 μm.

[8,21]. We also stained our samples for Ki-67 as a marker for cellular proliferation. Nine of 18 (47.4%) specimens examined exhibited at least one noncancerous area where CEP57 overexpression was found associated with basal cell hyperplasia. CEP57 was coexpressed with p63 in all of these samples, confirming that the cells overexpressing CEP57 are indeed basal cells (Figure 7). Of the nine basal cell hyperplasia regions with CEP57 overexpression, all exhibited strong staining for FGFR1, although only three of nine were positive for FGF-2 (Figure 7). When CEP57-positive basal cells were co-stained with the cellular proliferation marker Ki-67, we did not see a significant coincidence of the two proteins, underscoring that CEP57-overexpressing basal cells are largely non-proliferative.

CEP57 Expression Is Lost in Prostate Cancer Metastases

We next examined the expression of CEP57 in tissue specimens obtained from patients with mCRPC (Figure 8). Primary (n = 11) and metastatic (n = 5) prostate tumor specimens were collected from patients undergoing either palliative transurethral resection of the prostate or resection of a metastatic lesion (lymph node, n = 2; bone, n = 2, skin, n = 1). Of 11 samples from primary tumors, 7 (63.6%) showed CEP57 overexpression, whereas 4 samples (36.4%) showed low CEP57 expression (Figure 8A). Remarkably, all five (100%) of the metastatic lesions analyzed showed a loss of CEP57 protein expression (P < .05; Figure 8B).

Taken together, our results suggest that a high CEP57 expression has a negative impact of prostate cancer cell growth independent of AR nuclear trafficking and, furthermore, that CEP57 is frequently lost during malignant progression to a metastatic stage.

CEP57 Overexpression Impairs Cell Division

Having shown that overexpression of CEP57 does not block nuclear translocation of the AR, we performed a detailed microscopic analysis of CEP57-transfected cells to explain its negative effects on malignant progression without a strong reduction of tumor cell viability (Figure 3). CEP57-transfected cells were stained for α-tubulin to visualize microtubules.

We noticed an increase of cells with a disarranged microtubule network and abnormal nuclear morphology in comparison to controls (Figure 9A). These cells frequently contained two nuclei or sometimes three nuclei and showed a cytoplasmic indentation approximately in the midzone. A statistically significant three-fold increase of these cells was detected from 9.8% in controls to 29.6% in CEP57-overexpressing cells (P < .05).

Such a morphology has previously been described after cytokinesis failure, and we conclude that CEP57 induces mitotic dysfunction in a subset of cells that precludes the proper formation of daughter cells. Such effect could lead to a suppression of tumor cell proliferation, whereas the viability of cells, at least initially, is not strongly affected.

Discussion

Microtubule-dependent processes play a crucial role in normal and malignant cellular behavior [22]. CEP57 is a multifunctional protein that has been implicated in a number of microtubule-associated processes including microtubule nucleation and their anchoring at the centrosome as well as bundling of microtubules [7]. It has originally been identified as a crucial factor for the translocation of the 18-kDa isoform of FGF-2 (bFGF) into the nucleus [8,21]. CEP57 localizes to the centrosome and has furthermore been implicated in stable microtubule attachment at the centrosome and the kinetochore [17]. Recent results have shown that CEP57 forms a complex with the centrosomal proteins CEP63 and CEP152 [23] and that CEP57 can stimulate centrosome overduplication and mitotic defects through the aberrant stabilization of daughter centrioles [6]. We found that CEP57 is overexpressed in a subset of prostate cancers, a tumor entity in which FGF-2 signaling [24] and microtubule-dependent transport processes play pivotal roles in malignant progression.

In the present report, we show that, contrary to our expectations, high CEP57 expression is not associated with poor patient survival but instead is associated with a moderate but significant BCR-free survival advantage in a total of 525 prostate cancer patients analyzed in 2 independent cohorts. In line with this notion, we found a negative impact of CEP57 overexpression on prostate cancer cell viability and proper mitosis. However, a link between high CEP57 expression and nuclear transport of the AR due to aberrant microtubule bundling could not be corroborated. Instead, we found that AR transport remains normal in cells in which microtubule dynamics are highly altered by CEP57 overexpression. Furthermore, we discovered that CEP57 expression is frequently lost in prostate cancer metastases. Hence, our results suggest that negative growth-regulatory functions of CEP57 override its potentially oncogenic activities in prostate cancer, thus creating selection pressure for its loss.

It is important to mention in this context that CEP57 is not only a centrosomal protein but also a component of the central spindle and the midbody [25]. Depletion of CEP57 has previously been reported to negatively impact on cytokinesis through disruption of these structures, leading to an increase of binucleated cells [25]. Results shown here indicate that overexpression of CEP57 likewise affects proper cell division. Whether and how CEP57 overexpression causes mitotic
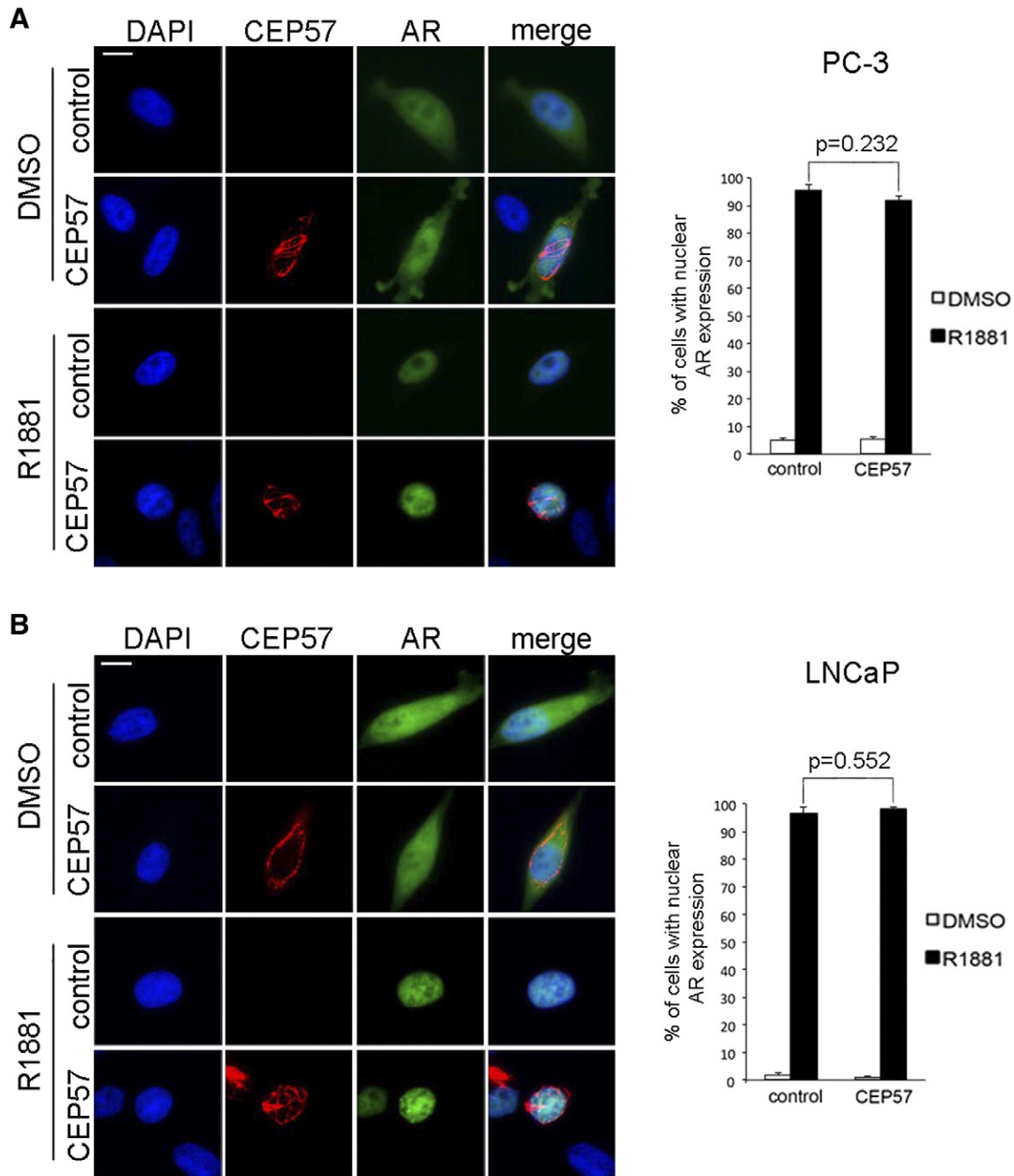
Figure 5. CEP57-induced microtubule bundling does not prevent AR nuclear translocation. (A, B) Fluorescence microscopic analysis of PC-3 (A) or LNCaP (B) cells following transfection with AR-GFP together with either empty vector (control) or mCEP57. Twenty-four hours after transfection, cells were treated with 5 nM R1881 or DMSO as a control for 2 hours to induce AR nuclear translocation. Note that microtubule bundling induced by CEP57, which decorates the "baskets," does not prevent nuclear translocation of AR-GFP. Nuclei stained with DAPI. Scale bar represents 10 μm. Bar graphs show mean and standard error of two independent experiments. *P* values were calculated using Student's two-tailed *t* test for independent samples.

dysfunction through a similar disruption of the central spindle and midbody remain to be determined. CEP57 has also been shown to be essential for spindle pole integrity [26], and disruption of this function due to its overexpression may likewise negatively affect daughter cell formation. In general, microtubules have been implicated in the regulation of contractility [27], and CEP57 may hence affect contractile ring formation during mitosis as another potential mechanism leading to mitotic impairment.

CEP57 overexpression has been found to lead to centrosome aberrations, which can promote chromosomal instability and malignant progression [6]. However, centrosome aberrations may not necessarily provide a growth advantage. In fact, it has previously been shown that centrosome amplification can hinder cell proliferation [28]. Hence, reduced proliferation and a decreased ability to generate viable daughter cells may stem from both centrosome amplification and other disturbances of microtubule homeostasis.
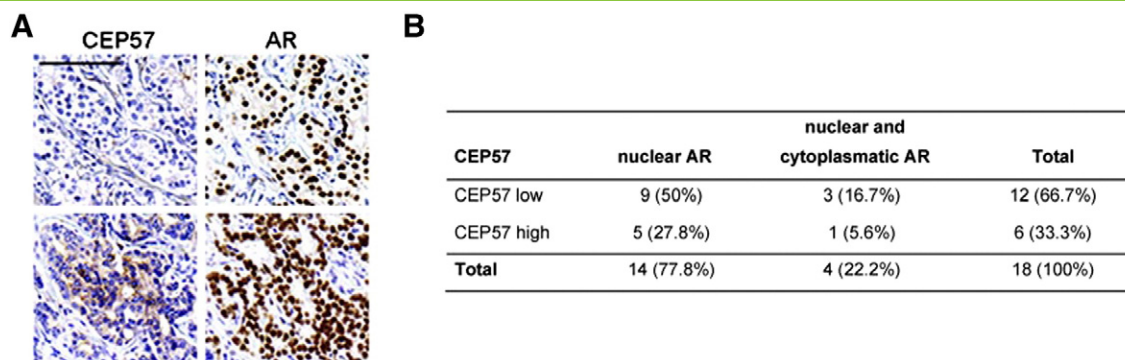
Figure 6. AR localization is not dependent on CEP57 overexpression *in vivo*. (A) Immunohistochemical analysis of prostate cancer specimens for CEP57 and AR. Note the presence of nuclear AR in tumors with high CEP57 expression. Scale bar represents 100 μm. (B) Overview of immunohistochemical staining results. No statistically significant correlation between CEP57 and AR expression was found (*P* > .05; Fisher exact probability test).

In more general terms, it is possible that mechanisms that promote chromosomal instability and mechanisms that negatively affect cellular proliferation are competing processes. With this respect, CEP57 overexpression may have different cellular consequences when compared with proteins such as PLK4, which is believed to have exclusively centrosomal functions [29,30]. Biallelic mutations of

Figure 7. CEP57 is overexpressed in prostate basal cells. Immunohistochemical analysis of directly adjacent tissue sections from a representative area with prostate basal cell hyperplasia (left panels) and prostate cancer (right panels) from the same prostatectomy specimen for CEP57, p63, FGF2, FGFR1, and Ki-67. Scale bar = 50 μm (left) or 100 μm (right).

CEP57 have been detected in a subset of patients with mosaic variegated aneuploidy syndrome [31], but how exactly loss of CEP57 leads to aneuploidy and cancer predisposition in these patients remains to be determined. Our finding that all metastatic lesions analyzed showed a loss of CEP57 expression together with the poor outcome of a patient with absence of CEP57 expression in TMA II (Figure 1), however, underscores that CEP57 loss of function can promote malignant progression, potentially through a number of mechanisms [17,25,26,32].

Although we could not corroborate a role of CEP57 in preventing nuclear translocation of the AR, a crucial process targeted by several anticancer agents in prostate cancer [15,19], this does not rule out that other transport cargoes may be responsible for the observed effects. For example, CEP57 has been reported to interact with cyclin D1 and to promote cellular quiescence by preventing nuclear accumulation of cyclin D1, thereby blocking CDK4-dependent phosphorylation of the retinoblastoma tumor suppressor (pRB) [32]. Conversely, CEP57 overexpression caused a reduction of cells in S phase [32]. When we performed a flow cytometric analysis of CEP57-transfected LNCaP cells, we did not find a significant reduction of S phase cells (not shown) pointing to cell-specific and/or dosage effects. However, we cannot rule out that this function of CEP57 also contributes to the less aggressive tumor growth characteristics associated with CEP57 overexpression *in vivo* and/or modulates the proliferative activity of prostate basal cells.

Taken together, the findings presented here underscore an association of high CEP57 expression with less aggressive tumor growth. This, together with our finding that even massive microtubule bundling induced by high CEP57 expression does not prevent AR nuclear translocation, has important translational implications. First, CEP57 could be used as a prognostic biomarker, ideally as part of a panel of markers, to stratify patients into risk categories. Second, the mode of action of microtubule-stabilizing drugs such as taxanes, which are widely used in advanced prostate cancer, may be independent from blocking AR trafficking. This suggests that hormonal therapy and taxanes function, at least in part, in a nonoverlapping fashion. Although further experiments to corroborate this are currently under way, recent results showing an impressive overall survival benefit from adding docetaxel to ADT in men with metastatic prostate cancer lend important support to this notion [33].

Supplementary data to this article can be found online at http://dx.doi.org/10.1016/j.tranon.2015.11.004.
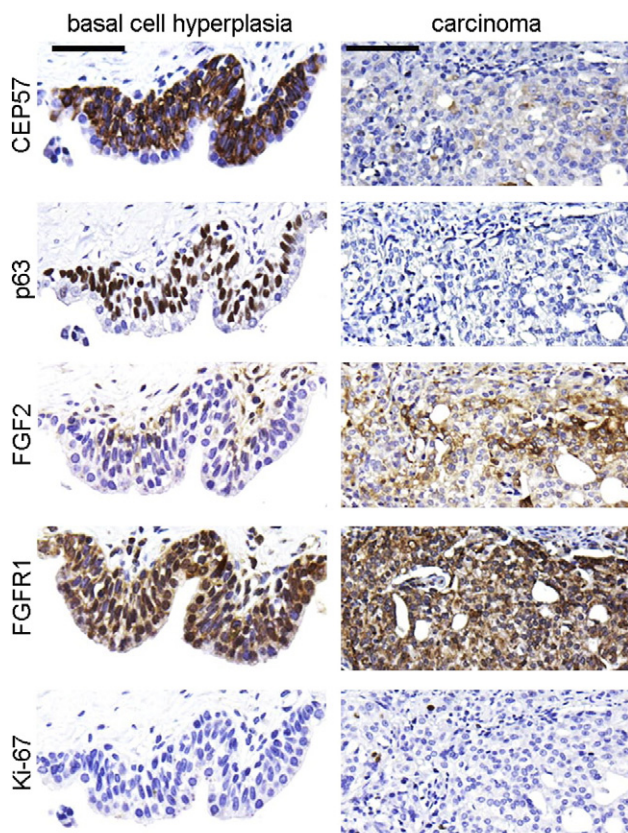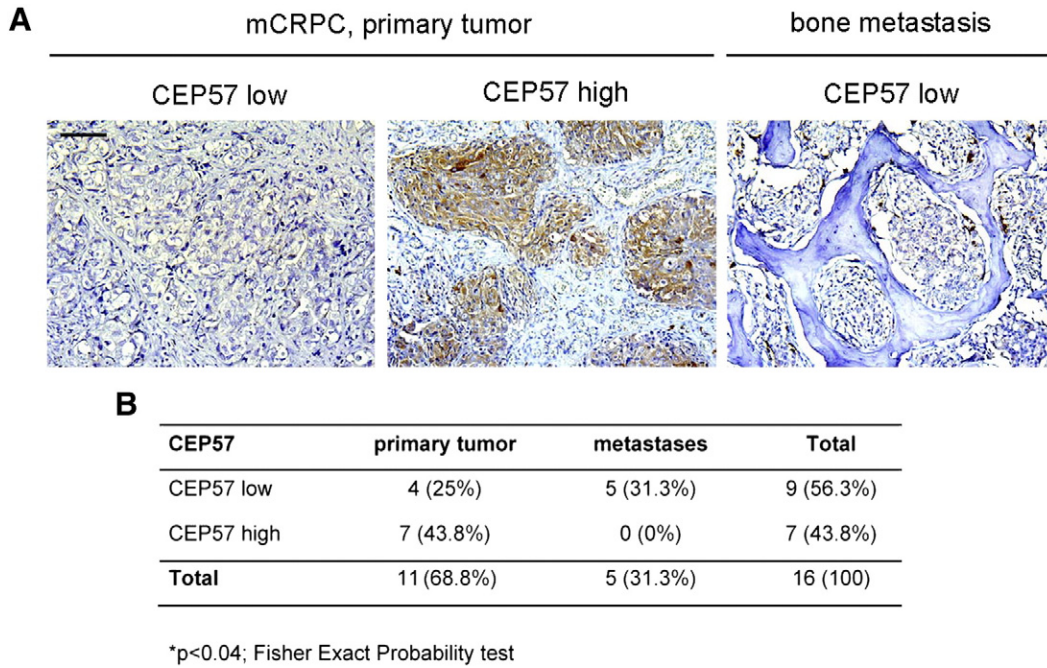
Figure 8. Loss of CEP57 expression in prostate cancer metastases. (A) Immunohistochemical analysis of tissue specimens from mCRPC or a bone lesion for CEP57. Scale bar = 50 μm. (B) Overview of staining results. Note the uniformly low expression of CEP57 in metastatic lesions.
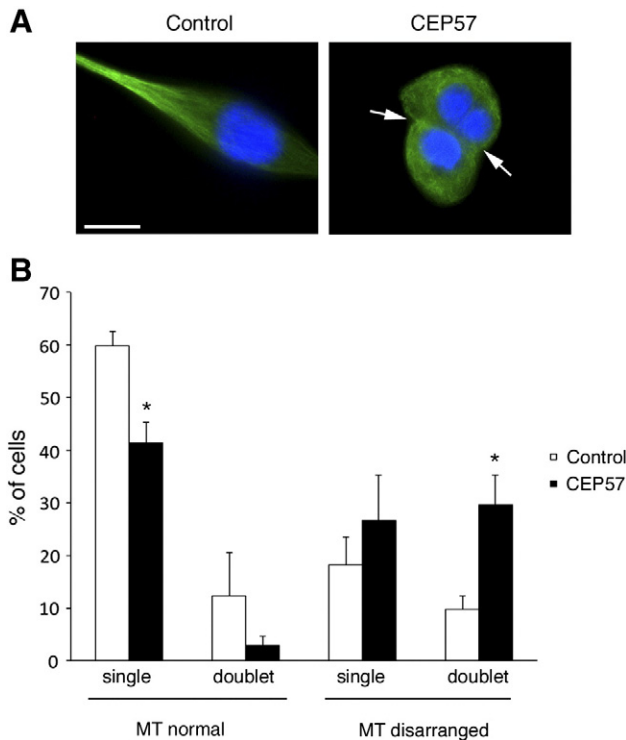

Figure 9. CEP57 overexpression impairs mitosis. (A) Immunofluorescence microscopic analysis of LNCaP cells transfected (48 hours) with empty vector (left, single cell) or CEP57 (right, doublet) using DsRED as transfection marker (channel not shown). Note the disarranged microtubule network in the CEP57-transfected cell and the cytoplasmic indentations (arrows). Nuclei are stained with DAPI. Scale bar = 10 μm. (B) Quantification of control or CEP57-transfected cells with normal or disarranged microtubule (MT) network and either showing a single nucleus or binucleation (doublet). Each bar represents mean and standard error of three independent experiments. Asterisks indicate statistical significance ($P < .05$).

References

[1] Siegel R, Naishadham D, and Jemal A (2013). Cancer statistics, 2013. *CA Cancer J Clin* **63**, 11–30.

[2] Schröder FH, Hugosson J, Roobol MJ, Tammela TLJ, Zappa M, Nelen V, Kwiatkowski M, Lujan M, Määttänen L, and Lilja H, et al (2014). Screening and prostate cancer mortality: results of the European Randomised Study of Screening for Prostate Cancer (ERSPC) at 13 years of follow-up. *Lancet* **384**, 2027–2035.

[3] Tapia-Laliena MA, Korzeniewski N, Hohenfellner M, and Duensing S (2014). High-risk prostate cancer: a disease of genomic instability. *Urol Oncol* **32**, 1101–1107.

[4] Duensing S (2005). A tentative classification of centrosome abnormalities in cancer. *Cell Biol Int* **29**, 352–359.

[5] Pihan GA, Purohit A, Wallace J, Malhotra R, Liotta L, and Doxsey SJ (2001). Centrosome defects can account for cellular and genetic changes that characterize prostate cancer progression. *Cancer Res* **61**, 2212–2219.

[6] Cuevas R, Korzeniewski N, Tolstov Y, Hohenfellner M, and Duensing S (2013). FGF-2 disrupts mitotic stability in prostate cancer through the intracellular trafficking protein CEP57. *Cancer Res* **73**, 1400–1410.

[7] Momotani K, Khromov AS, Miyake T, Stukenberg PT, and Somlyo AV (2008). Cep57, a multidomain protein with unique microtubule and centrosomal localization domains. *Biochem J* **412**, 265–273.

[8] Bossard C, Laurell H, Van den Berghe L, Meunier S, Zanibellato C, and Prats H (2003). Translokin is an intracellular mediator of FGF-2 trafficking. *Nat Cell Biol* **5**, 433–439.

[9] Balk SP and Knudsen KE (2008). AR, the cell cycle, and prostate cancer. *Nucl Recept Signal* **6**e001.

[10] Heinlein CA and Chang C (2004). Androgen receptor in prostate cancer. *Endocr Rev* **25**, 276–308.

[11] Yap TA, Zivi A, Omlin A, and de Bono JS (2011). The changing therapeutic landscape of castration-resistant prostate cancer. *Nat Rev Clin Oncol* **8**, 597–610.

[12] Sharma NL, Massie CE, Ramos-Montoya A, Zecchini V, Scott HE, Lamb AD, MacArthur S, Stark R, Warren AY, and Mills IG, et al (2013). The androgen

receiver induces a distinct transcriptional program in castration-resistant prostate cancer in man. *Cancer Cell* **23**, 35–47.

[13] Antonarakis ES, Lu C, Wang H, Luber B, Nakazawa M, Roeser JC, Chen Y, Mohammad TA, Chen Y, and Fedor HL, et al (2014). AR-V7 and resistance to enzalutamide and abiraterone in prostate cancer. *N Engl J Med* **371**, 1028–1038.

[14] Arora VK, Schenkein E, Murali R, Subudhi SK, Wongvipat J, Balbas MD, Shah N, Cai L, Efstathiou E, and Logothetis C, et al (2013). Glucocorticoid receptor confers resistance to antiandrogens by bypassing androgen receptor blockade. *Cell* **155**, 1309–1322.

[15] Thadani-Mulero M, Nanus DM, and Giannakakou P (2012). Androgen receptor on the move: boarding the microtubule expressway to the nucleus. *Cancer Res* **72**, 4611–4615.

[16] Piel M, Meyer P, Khodjakov A, Rieder CL, and Bornens M (2000). The respective contributions of the mother and daughter centrioles to centrosome activity and behavior in vertebrate cells. *J Cell Biol* **149**, 317–330.

[17] Emanuele MJ and Stukenberg PT (2007). Xenopus Cep57 is a novel kinetochore component involved in microtubule attachment. *Cell* **130**, 893–905.

[18] Scher HI, Fizazi K, Saad F, Taplin M-E, Sternberg CN, Miller K, de Wit R, Mulders P, Chi KN, and Shore ND, et al (2012). Increased survival with enzalutamide in prostate cancer after chemotherapy. *N Engl J Med* **367**, 1187–1197.

[19] Darshan MS, Loftus MS, Thadani-Mulero M, Levy BP, Escuin D, Zhou XK, Gjyrezi A, Chanel-Vos C, Shen R, and Tagawa ST, et al (2011). Taxane-induced blockade to nuclear accumulation of the androgen receptor predicts clinical responses in metastatic prostate cancer. *Cancer Res* **71**, 6019–6029.

[20] Sailer V, Stephan C, Wernert N, Perner S, Jung K, Dietel M, and Kristiansen G (2013). Comparison of p40 (ΔNp63) and p63 expression in prostate tissues—which one is the superior diagnostic marker for basal cells? *Histopathology* **63**, 50–56.

[21] Meunier S, Navarro MG-J, Bossard C, Laurell H, Touriol C, Lacazette E, and Prats H (2009). Pivotal role of translokin/CEP57 in the unconventional secretion versus nuclear translocation of FGF2. *Traffic* **10**, 1765–1772.

[22] Kavallaris M (2010). Microtubules and resistance to tubulin-binding agents. *Nat Rev Cancer* **10**, 194–204.

[23] Lukinavičius G, Lavogina D, Orpinell M, Umezawa K, Reymond L, Garin N, Gönczy P, and Johnsson K (2013). Selective chemical crosslinking reveals a Cep57-Cep63-Cep152 centrosomal complex. *Curr Biol* **23**, 265–270.

[24] Corn PG, Wang F, McKeehan WL, and Navone N (2013). Targeting fibroblast growth factor pathways in prostate cancer. *Clin Cancer Res* **19**, 5856–5866.

[25] He R, Wu Q, Zhou H, Huang N, Chen J, and Teng J (2013). Cep57 protein is required for cytokinesis by facilitating central spindle microtubule organization. *J Biol Chem* **288**, 14384–14390.

[26] Wu Q, He R, Zhou H, Yu AC, Zhang B, Teng J, and Chen J (2012). Cep57, a NEDD1-binding pericentriolar material component, is essential for spindle pole integrity. *Cell Res* **22**, 1390–1401.

[27] Cinnamon Y, Feine O, Hochegger H, Bershadsky A, and Brandeis M (2009). Cellular contractility requires ubiquitin mediated proteolysis. *PLoS One* **4**e6155.

[28] Sato N, Mizumoto K, Nakamura M, Maehara N, Minamishima YA, Nishio S, Nagai E, and Tanaka M (2001). Correlation between centrosome abnormalities and chromosomal instability in human pancreatic cancer cells. *Cancer Genet Cytogenet* **126**, 13–19.

[29] Cunha-Ferreira I, Rodrigues-Martins A, Bento I, Riparbelli M, Zhang W, Laue E, Callaini G, Glover DM, and Bettencourt-Dias M (2009). The SCF/Slimb ubiquitin ligase limits centrosome amplification through degradation of SAK/PLK4. *Curr Biol* **19**, 43–49.

[30] Habedanck R, Stierhof Y-D, Wilkinson CJ, and Nigg EA (2005). The Polo kinase Plk4 functions in centriole duplication. *Nat Cell Biol* **7**, 1140–1146.

[31] Snape K, Hanks S, Ruark E, Barros-Núñez P, Elliott A, Murray A, Lane AH, Shannon N, Callier P, and Chitayat D, et al (2011). Mutations in CEP57 cause mosaic variegated aneuploidy syndrome. *Nat Genet* **43**, 527–529.

[32] Ruiz-Miró M, Colomina N, Fernández RMH, Garí E, Gallego C, and Aldea M (2011). Translokin (Cep57) interacts with cyclin D1 and prevents its nuclear accumulation in quiescent fibroblasts. *Traffic* **12**, 549–562.

[33] Sweeney CJ, Chen Y-H, Carducci M, Liu G, Jarrard DF, Eisenberger M, Wong Y-N, Hahn N, Kohli M, and Cooney MM, et al (2015). Chemohormonal therapy in metastatic hormone-sensitive prostate cancer. *N Engl J Med* **373**, 737–746.